Journal of Hydroscience and Hydraulic Engineering
Vol. 15, No. 1, June, 1997, 1-9

GEOMETRY AND MIGRATION CHARACTERISTICS OF SAND BARS IN MEANDERING CHANNEL

By

Y. Shimizu and M. Fujita

Hokkaido University, Sapporo, Japan,

and

M. Hirano

Hokkaido Development Agency, Tokyo, Japan

SYNOPSIS

Geometric and migration characteristics of bar in meandering channel are investigated. Depth-averaged flow model coupled with bed deformation model is applied to meandering channels with a wide range of hydraulic and geometric conditions. From the results of the numerical experiment, a series of figures are presented, which show the effects of each parameter to the bar migration characteristics and finite amplitude bed topography. An empirical formula is proposed to estimate the finite amplitude bar height.

INTRODUCTION

Prediction of finite amplitude bed topography in a given hydraulic and geometric condition is an important subject in river engineering works. Among the various scales of bed forms of alluvial channels, this paper mainly deal with the meso-scale bed form, in which the characteristic length is represented by flow depth, channel width, or meandering wave length of channel geometry. Free bars, like alternate bars and forced bars in bends, are very important factors to determine the meso-scale bed configuration of rivers. These two phenomena have been discussed in many previous studies. Investigations of the interaction between free and forced bars, were pioneered by Kinoshita and Miwa(1). Hasegawa and Yamaoka(2) applied a quantitative treatment. This was followed by theoretical methods in which both free and forced bars develop resonantly at a given frequency of meandering channels, like in the theoretical studies by Blondeaux and Seminara(3) and by Parker and Johannesson(4).

Numerical models have also been proposed by several researchers, e.g., Nelson and Smith(5), Shimizu and Itakura(6), to predict meso-scale bed configuration of meandering channels. It seems that most of the previous studies have succeeded to predict bed topography to a certain extent, however, these studies have only concerned with some limited condition of flow and channel geometry. In this paper, a series of numerical experiments are conducted while each

parameters such as non-dimensional meander wavelength, non-dimensional maximum curvature and non-dimensional width of the channel are changed individually. The finite amplitude bed topography in each condition is calculated, and the effect of each parameter on finite bed topography as well as the migration characteristics of bar is clarified. Through this study, general characteristics of meso-scale bed topography is summarized more comprehensively than the previous studies. Based on all the calculated and experimental results, an empirical formula to predict finite amplitude bar height is proposed.

PROCEDURE OF STUDY

In this paper, the notation symbols denote non-dimensional values, and dimensional ones are expressed with ~. The mathematical model used in this study is a semi-three-dimensional numerical model of flow and bed deformation proposed by Shimizu et al.(7), which have been verified in terms of various experimental results. The channel geometry is represented by sine-generated curve along the non-dimensional axis s normalized by half channel width $\tilde{B}$ as;

$$\varphi = \varphi_0 \cos\left(\frac{2\pi}{L}s\right) \tag{1}$$

in which s = axis along the channel centerline ($=\tilde{s}/\tilde{B}$); φ = meander angle; L = meander wave length of channel along s axis ($=\tilde{L}/\tilde{B}$); and φ_0 = value of φ at $\tilde{s}=0$.

The channel geometry, and flow and bed conditions can be represented by the following normalized parameters of channel meander wave number λ, maximum channel curvature ν, channel width β, grain size diameter d_s, shear stress τ_{*0} and Froude number F_r.

$$\lambda = 2\pi\frac{\tilde{B}}{\tilde{L}} \quad \nu = \frac{\tilde{B}}{\widetilde{R_0}} \quad \beta = \frac{\tilde{B}}{\widetilde{D_0}} \quad d_s = \frac{\widetilde{d_s}}{\widetilde{D_0}} \qquad \tau_{*0} = \frac{\widetilde{D_0}S_f}{\left(\frac{\rho_s}{\rho}-1\right)\widetilde{d_s}} \quad F_r = \frac{\widetilde{U_0}}{\sqrt{\tilde{g}\widetilde{D_0}}} \tag{2}$$

in which $\widetilde{R_0}$ = the minimum radius of curvature of channel; $\widetilde{D_0}$ = averaged depth; $\widetilde{d_s}$ = diameter of bed material; $\widetilde{U_0}$ = mean velocity of flow; $\tilde{g}$ = the acceleration of gravity; S_f = averaged channel slope in flow direction; $\widetilde{\rho_s}$ = density of bed material; and $\tilde{\rho}$ = density of water.

Among the six parameters defined by Eq. 2, λ and ν represents the channel geometry, β represents the channel cross-sectional shape, d_s represents the bed roughness through the bed material size, τ_{*0} represents the quantity of bed load, and F_r represent the flow regime. Most of the given condition of flow and geometry can be expressed by the combination of these parameters. L and φ_0 in Eq. 1 can be described in terms of λ and ν as,

$$L = \frac{2\pi}{\lambda} \qquad \varphi_0 = \frac{\nu L}{2\pi} \tag{3}$$

By the combination of λ and ν, various channel geometry can be specified as shown in Fig. 1. Straight channels are defined as ν=0 and L=∞, resulting λ=0 using the relation of Eq. 3.

In order to investigate the characteristics of bed topography and bar migration depending on the channel geometry, λ, ν and β are chosen as parameters for the sensitivity analysis. Combination of 5 values of λ and 6 values of ν represents 30 channel geometry as shown in Fig.1. Over each geometry shown in Fig. 1, four different values of β (5, 10, 15, 20) are applied,

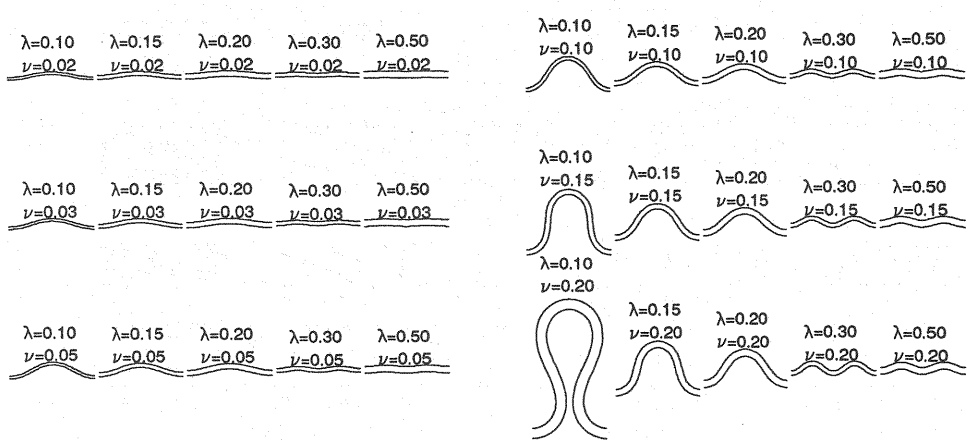

Fig. 1 Plane geometry of test channels by combination of *lambda* and ν

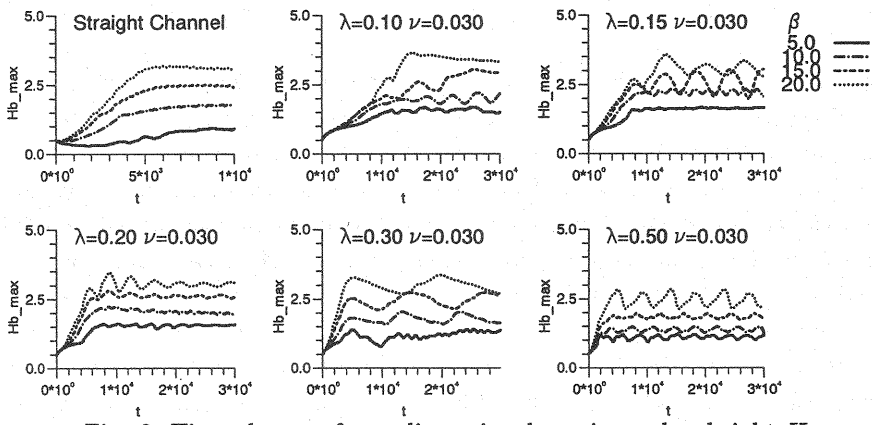

Fig. 2 Time change of non-dimensional maximum bar height H_b
($\nu = 0.03$, $\lambda = 0.1 \sim 0.5$, $\beta = 5 \sim 20$)

and thus 120 series of numerical experiments are conducted in this study. In order to test the pure effect of λ, ν and β, the other parameters are kept constant as $d_s = 0.05$, $\tau_{*0} = 0.08$ and $F_r = 0.83$. Conditions with $\beta = 10, 15$ and 20 are classified in alternate bar condition according to regime criteria proposed by Kuroki and Kishi(8), while $\beta = 5$ is classified in no-bar condition.

MIGRATION CHARACTERISTICS OF BAR

Series of numerical experiments were conducted until steady bed topography was obtained under the condition defined in the previous section. Most of the calculated results reached equilibrium state after some calculations, however, depending on parameters, calculated results showed some oscillating movement. For example, Fig 2 show the time dependent variation of calculated maximum non-dimensional bar height, H_b, when $\nu = 0.03$. In which, H_b is the difference between highest and lowest bed elevation over the channel with the set up condition. Horizontal axis of Fig 2, t is the non-dimensional time, $t = \tilde{t} \cdot \widetilde{U_0}/\widetilde{B}$, in which $\tilde{t}$ is the time.

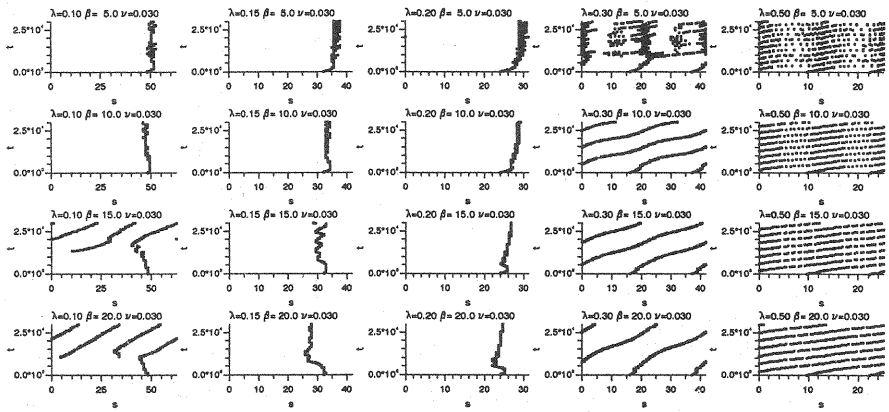

Fig. 3 Time change of most eroded point along test channels
($\nu = 0.03$, $\lambda = 0.1 \sim 0.5$, $\beta = 5 \sim 20$)

In every result of Fig 2, H_b tends to increase with the increase of β. H_b becomes stable when the value of $\lambda = 0.2$, however, showing an oscillating nature in other cases. The amplitude of the oscillation is smaller when β is small. In order to see the relation between the oscillation and bar migration, temporal change of the deepest point in each calculation is plotted in Fig. 3. The horizontal axis of Fig. 3 is non-dimensional longitudinal axis s, and each line shows the temporal change of the deepest point along left-hand side bank. Bar migration is not observed when $\lambda = 0.15$ and 0.20, and it takes place when $\lambda = 0.30$ and 0.50. The migration velocity is faster when the value of λ becomes more distant from the value of $\lambda = 0.15$ and 0.20. The examples shown in Fig.3 are data of channels with very gentle curvature as $\nu = 0.03$. It seems that one wave length of free bar fits into one wave length of channel meander when λ=0.15 $\sim$ 0.2. On the contrary, when $\lambda = 0.1$, bar starts to migrate with increase of β which amplifies the migration characteristics of free bar.

The temporal change of the most eroded point is shown in Fig. 4 when the curvature of meander is large as $\nu = 0.2$. In this case, since the effect of channel curvature is dominant, bar migration is not seen in most cases. It is only observed when $\lambda = 0.5$ and $\beta = 20$, in which meander wave length is very small and free bar effect is dominant. In this case, free bar can propagate through the channel meander. Plural eroded points in one meander wavelength are observed when λ=0.1. It is because that the meander wave length of channel geometry is much longer than that of free bar, and more than one free bar can exist in one channel meander.

Kinoshita and Miwa(1) had proposed a regime criteria for the bar migration from a large number of experimental data. All the results of numerical experiments in this study are plotted in Kinoshita and Miwas' figure in Fig. 5.

The vertical axis and horizontal axis of Fig. 5 are $\tilde{\ell}/2\tilde{b}$ ($\tilde{\ell}$ is meander wave length and $\tilde{b}$ is channel width) and 2θ (θ is meander angle), respectively, which can be represented using the non-dimensional parameters as $\pi/2\lambda$ and $2\nu/\lambda$, respectively.

In the symbols of Fig. 5, $\bigcirc$ denotes the bar migration regardless with the value of β and $\times$ denotes no migration. $\triangle$ and $\square$ are the experiments with bar migration when β is larger than 15 and 20, respectively. All the results generally agree with Kinoshita and Miwas' criteria, however, in the neighborhood area of the Kinoshita and Miwas' curve, bar migration is only

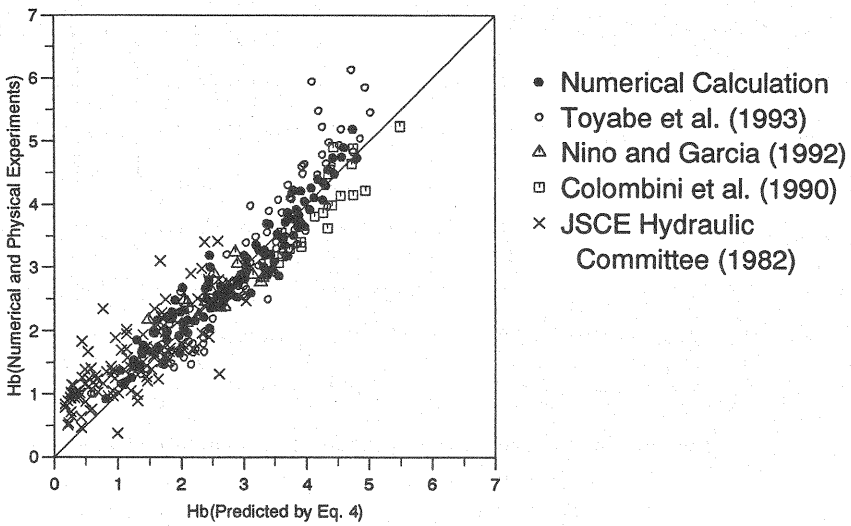

Fig. 8 Comparison of bar height between Eq.(4) and numerical experiments and physical experiments

$$H_b = \left\{1.0 + 0.1\Omega + (-18.4 + 15.6\Omega - 2.5\Omega^2 + 0.12\Omega^3)\nu \right. \\ \left. +(0.1 - 0.004\Omega)\beta\right\}(0.3 + 19.0d_s - 88.1d_s^2) \qquad (4)$$

in which $\Omega = 1/\lambda$ and d_s = non-dimensional grain size of bed material normalized by averaged flow depth. Parameter d_s is introduced because it is another important parameter for the prediction of H_b [Shimizu et. al (7)]. All the results of numerical experiment in this study are compared with Eq. 4 with symbol ● in Fig. 8. In the figure, experimental results by Toyabe et. al(9), ○, Nino and Garcia(10), △, Colombini et. al(11), and experimental data summarized by JSCE (12), ×, are also plotted. Some data by Toyabe et al., ○, show disagreements with Eq. 4. These experiments are with condition of β=20, in which multi row bar is developed in the channel. Except these, the data shows the good agreement with Eq. 8.

CONCLUSION

Large number of numerical calculations were conducted to investigate the finite amplitude bed topography in meandering channels with a wide range of geometric and hydraulic condition. Some important characteristics to determine the bed topography and bar migration are clarified, including the critical meander angle at which the free bar cease to migrate. Using the data set obtained from the numerical experiments, a practical formula to predict finite amplitude bar height is proposed. The formula is verified using the data obtained from numerical calculations as well as large number of experimental results. It was shown that the finite amplitude bar height can be predicted to some extent by a simple formula without complex calculation or physical experiment.

This study is supported by Foundation of Hokkaido River Disaster Prevention Research Center.

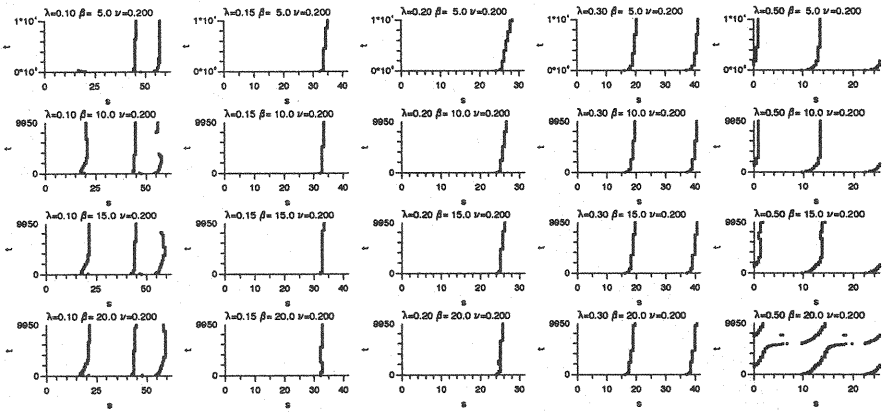

Fig. 4 Time change of most eroded point along test channels
($\nu = 0.2$, $\lambda = 0.1 \sim 0.5$, $\beta = 5 \sim 20$)

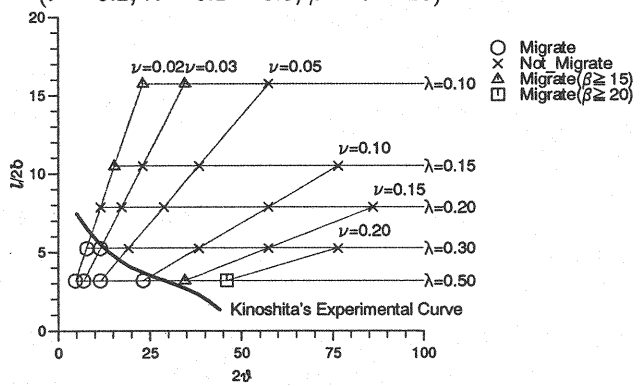

Fig. 5 Criteria for bar migration

seen when the value of β is large. Bar migration is also seen in the potion far from the curve as symbols of $\triangle$ ($\lambda = 0.10$ and ν=0.02$\sim$0.03). In these cases, free bars are not trapped by the channel meander, but they pass through the channel bends.

NON-DIMENSIONAL BAR HEIGHT

Among various parameters of bed topography, bar height is one of the most important parameter from the view point of river engineering. From the series of numerical experiments in this study, relationship between finite amplitude bar height H_b and other hydraulic parameters are discussed. When the bar height shows an oscillating nature in time as shown in Fig. 2, finite amplitude bar height is defined as the maximum bar height.

Fig. 6 shows the relation among H_b, ν, λ and β, in which each panel shows the results in terms of different ν. λ=0 denotes the straight channels. In every panel of Fig. 6, peaks of H_b is seen when λ=0.1$\sim$0.2, and these are higher when ν is larger. These suggest the occurrence of resonance between free and forced bars. The resonance is not very dominant when the value of ν is small and it becomes remarkable with the increase of ν. H_b tends to increase with increase of β, and this tendency is more conspicuous when ν is large. These characteristics can be explained as, the development of free bar is promoted by increase of β, however, it is

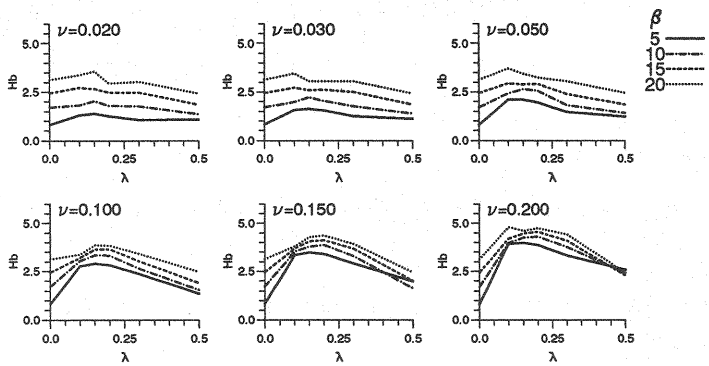

Fig. 6 Relationship among H_b, β, ν and λ in meandering channels

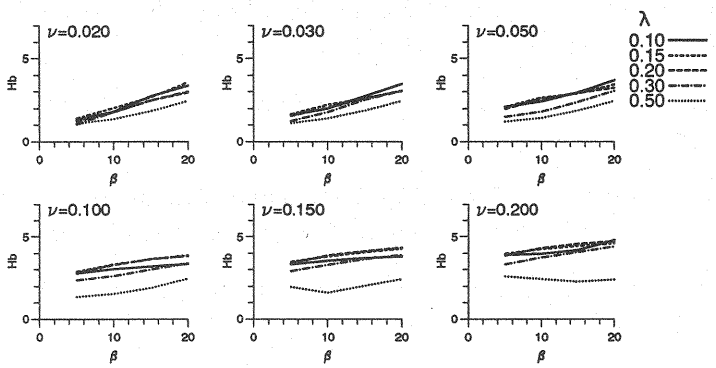

Fig. 7 Relationship among H_b, β, ν and λ in meandering channels

restrained by the effect of forced bar with the increase of ν. And it can be summarized that the growth of finite amplitude bar height is controlled primarily by the basic linear effect of ν, and effect of channel bend, and is damped or promoted nonlinearly by the effect of λ and β.

Fig 7. shows the relation of H_b and β, in which the data are the same as in Fig. 6. H_b is linearly increasing with increase of β, in which the ratio of increase is larger when ν is small. It is suggested that the effect of β on H_b is almost linear, and it is slightly depressed by the combination of ν and λ, which represents the channel geometry.

PRACTICAL FORMULA OF BAR HEIGHT

The finite amplitude bar height is affected by both the geometric and free bar effect, as mentioned in the previous section. The prediction of finite amplitude bar height therefore can be enabled only when the time dependent calculations are conducted taking into account for these nonlinear effects. However, a practical formula to predict the finite amplitude bar height is desired from engineering purposes. Taking into account for the characteristics of ν, λ and H_b shown in Fig. 7 and 8, the following empirical formula to predict H_b is proposed.

REFERENCES

1. Kinoshita, R. and Miwa: River channel formation which prevents downstream movement of transverse bars, Shin-Sabo, Vol94, pp.12–17, 1974 (in Japanese).

2. Hasegawa, K. and Yamaoka: The Effect of plane and bed forms of channels upon the meander development, Proc. JSCE, Vol229, pp.143–152, 1980.

3. Blondeaux, P. and Seminara: A unified bar-bend theory of river meanders, J. Fluid Mech. 157, pp.449–470, 1985.

4. Johannesson, H. and Parker, G.: Secondary flow in mildly sinuous channel, J. Hydr. Engrg., ASCE, 115(3), pp.289–308, 1989.

5. Nelson, J.M. and J.D. Smith: Evolution and Stability of Erodible Channel Beds, River Meandering, AGU Monograph No. 12, pp.379–415, 1989.

6. Shimizu, Y. and T. Itakura: Calculation of bed variation in alluvial channels, J. Hydr. Engrg., ASCE, 115(3), pp.367–384, 1990.

7. Shimizu, Y., Y. Watanabe, and T. Toyabe: Finite Amplitude Bed Topography in Straight and Meandering Rivers, Proc. JSCE, No.509/II-30, pp.67–78, 1995 (in Japanese).

8. Kuroki, M. and T. Kishi: Regime Criteria on Bars and Braids in Alluvial Straight Channels, Proc., JSCE, No.342, pp.87–96, 1984 (in Japanese).

9. Toyabe, T., Y. Watanabe, and Y. Shimizu: Movable Bed Experiments on Overdeepning by Resonance in Meandering Channel, Proc., JSCE, Hokkaido Div. No. 49, pp.433–438, 1993 (in Japanese).

10. Nino, Y. and M. Garcia: Sediment Bars in Straight and Meandering Channels, Experimental Study on the Resonance Phenomenon, Civil Engineering Studies, Hydraulic Engineering Series No. 42, University of Illinois at Urbana-Champaign, pp.1–118, 1992.

11. Colombini, M., M. Tubino and P. Whiting: Topographic Expression of Bars in Meandering Channels, Third International Workshop on Gravel-Bed Rivers, Florence, 24-28 September, 1990.

12. JSCE Hydraulic Committee: Three-dimensional Flow and Bed Forms in Rivers, pp.1–86, 1982 (in Japanese).

APPENDIX – NOTATION

The following symbols are used in this paper:

$\widetilde{B}$	=	half channel width;
$\widetilde{D_0}$	=	averaged depth;
$\widetilde{b}$	=	channel width;
d_s	=	normalized grain size diameter;
$\widetilde{d_s}$	=	diameter of bed material;
F_r	=	Froude number;
$\widetilde{L}$	=	meander wave length;
L	=	normalized meander wave length of channel along s axis;
$\widetilde{\ell}$	=	meander wave length;
$\widetilde{g}$	=	acceleration of gravity;
H_b	=	the maximum non-dimensional bar height;
$\widetilde{R_0}$	=	the minimum radius of curvature of channel;
S_f	=	averaged channel slope in flow direction;
s	=	axis along the channel centerline;
t	=	non-dimensional time;
$\widetilde{U_0}$	=	mean velocity of flow;
β	=	normalized channel width;
λ	=	normalized channel meander wave number;
ν	=	normalized maximum channel curvature;
$\widetilde{\rho}$	=	density of water;
$\widetilde{\rho_s}$	=	density of bed material;
τ_{*0}	=	normalized bed shear stress;
φ	=	meander angle;
φ_0	=	value of φ at $\widetilde{s} = 0$; and
Ω	=	$1/\lambda$.

(Received January 11, 1996; revised July 1, 1997)